Feedback-controlled running holograms in strongly absorbing photorefractive materials

J. Frejlich, A. A. Freschi,* and P. M. Garcia†

Laboratório de Óptica, Instituto de Física, Universidade Estadual de Campinas, Caixa Postal 6165, 13083-970 Campinas—SP, Brazil

E. Shamonina, V. Ya. Gayvoronsky,‡ and K. H. Ringhofer

Department of Physics, University of Osnabrück, D-49069 Osnabrück, Germany

Received July 14, 1999; revised manuscript received May 10, 2000

We propose a mathematical model for the movement in absorbing materials of photorefractive holograms under feedback constraints. We use this model to analyze the speed of a fringe-locked running hologram in photorefractive sillenite crystals that usually exhibit a strong absorption effect. Fringe-locked experiments permit us to compute the quantum efficiency for the photogeneration of charge carriers in photorefractive crystals if the effect of bulk absorption and the effective value of the externally applied field are adequately taken into consideration. A $Bi_{12}TiO_{20}$ sample was measured with the 532-nm laser wavelength, and a quantum efficiency of $\Phi = 0.37$ was obtained. Disregarding absorption leads to large errors in Φ. © 2000 Optical Society of America [S0740-3224(00)00209-5]

OCIS codes: 160.5320, 190.7070, 160.2900, 050.7330.

1. INTRODUCTION

Absorption effects are inherent in all photorefractive crystals and introduce serious difficulties in the mathematical formulation of the movement of holograms under feedback constraints. The movement of a hologram depends on the speed of recording and erasure, which in turn depend on the Maxwell or dielectric relaxation time.[1,2] The relaxation time in these materials depends on the intensity of light at the point where the measurement is carried out and, for absorbing materials, varies with the thickness of the material. The feedback condition is based on a macroscopic parameter at the crystal output. This parameter has a complicated mathematical relation with the thickness-dependent response time in the crystal and leads to an experimental difficulty. An experimental difficulty arises from the fact that whenever an external electric field is applied to the crystal, as is usually done in most experiments, its effective value at the point where measurements are carried out is not well known because of the photoconductive nature of these materials and because it is impossible that a truly uniform pattern of light is projected on the crystal. If there is some spatial variation in the light intensity along the direction between the two electrodes, either because the intensity profile of the incident beam or because of crystal edge shadowing, multiple interference effects, etc., the (photo)conductivity inside the crystal will vary accordingly and the field inside the crystal will no longer be able to be computed as the voltage-over-interelectrode distance.

It has already been shown[3] that the speed of a photorefractive fringe-locked (a particular kind of feedback-controlled) running hologram depends on the quantum efficiency of charge-carrier generation (Φ) as well as on the mobility–lifetime ($\mu\tau$) product of these carriers. As was pointed out above, the presence of bulk absorption introduces additional difficulties into the mathematical analysis of these holograms and makes them dependent on the effective density of photoactive centers $[(N_D)_{\text{eff}}]$. These photoactive centers can be obtained from steady-state stationary phase-shift experiments,[4] whereas $\mu\tau$ can be computed from initial hologram phase-shift experiments.[5] Once $\mu\tau$ and $(N_D)_{\text{eff}}$ are known, a fringe-locked running hologram experiment may provide an excellent means with which to compute the quantum efficiency, provided that a mathematical model is available that takes into account the influence of the bulk light absorption and the effective value of the applied electric field.

2. THEORY: FRINGE-LOCKED RUNNING HOLOGRAMS IN ABSORBING CRYSTALS

A mathematical description of feedback-controlled running holograms has been published before,[3,6] but its formulation in absorbing materials, as discussed above, needs a more detailed analysis.

A. Fringe-Locked Running Holograms

The interference of two mutually coherent and slightly detuned beams yields a light pattern that moves along the direction of the pattern wave vector with a speed that depends on the extent of detuning. When this pattern is projected onto a photorefractive material a hologram is produced that, in steady state, moves synchronously with the light pattern. The hologram's strength (diffraction efficiency) depends on its speed.[1,7] It is also possible to generate a photorefractive running hologram by use of a feedback-controlled technique: The phase shift φ be-

tween the transmitted and the diffracted beams propagating in the same direction behind the crystal is kept fixed at an arbitrarily chosen value that is different from the one that arises from a stationary hologram.[3,6] In this case the steady-state speed of the running hologram (and of the automatically attached light pattern) is determined by the degree of phase mismatch, the response time of the hologram, and the value of other experimental and material parameters. The response time of the hologram is proportional to the Maxwell relaxation time τ_M, which in turn is inversely proportional to the average light intensity.

A recent paper[8] has called attention to the asymmetric relation between the diffraction efficiency and the speed of the running hologram. Such asymmetry was shown to arise from the dependence of the Maxwell relaxation time on the average irradiance and on its variation along the sample thickness as a result of bulk absorption. One may wonder whether absorption also affects the feedback-controlled photorefractive running hologram and whether the value of the material parameters that can be computed from these experiments is also affected.

The generation of feedback-controlled running holograms has been described in detail elsewhere: One of the interfering beams is phase modulated with a small amplitude $\psi_d \approx 0.45$ rad and an angular frequency $\Omega = 2\pi 1700$ rad/s that is much larger than the frequency response of the hologram. Because of the nonlinear relation between phase and amplitude, the intensity of the beam along each of the two directions behind the crystal exhibits a harmonic term in Ω, where the amplitudes of the first and the second harmonics in Ω are, respectively,[3]

$$I_\Omega = 4J_1(\psi_d)\sqrt{I_R^0 I_S^0}\sqrt{\eta(1-\eta)}\sin\varphi, \tag{1}$$

$$I_{2\Omega} = 4J_2(\psi_d)\sqrt{I_R^0 I_S^0}\sqrt{\eta(1-\eta)}\cos\varphi. \tag{2}$$

A factor that accounts for the polarization relation between the transmitted and the diffracted beams behind the crystal should have been included in Eqs. (1) and (2). In our case, however, these beams are roughly parallel polarized (see details in Section 3 below), in which case this factor is approximately 1. These signals are detected with lock-in amplifiers tuned to Ω and 2Ω, respectively, and the corresponding output signals are amplified in such a way that

$$V_\Omega = A\sqrt{\eta(1-\eta)}\sin\varphi, \qquad V_{2\Omega} = A\sqrt{\eta(1-\eta)}\cos\varphi, \tag{3}$$

where η is the diffraction efficiency and A depends on the photodetectors, the irradiance of the incident recording beams, and the polarization, the phase amplitude modulation, and other experimental settings. The phase shift φ between the diffracted and the transmitted beams behind the sample can easily be computed from

$$\tan\varphi = V_\Omega/V_{2\Omega} \tag{4}$$

and is formulated in terms of material parameters[9] as

$$\sin\varphi = \frac{1}{2}\frac{\sinh(\Gamma d/4) - \cosh(\Gamma d/4)}{[\cosh^2(\Gamma d/4) - \cos^2(\gamma d/4)]^{1/2}}\sin\left(\frac{\gamma d}{2}\right), \tag{5}$$

for $I_R^0/I_S^0 \gg 1$, with

$$\Gamma = -\frac{2\pi n^3 r_{\text{eff}}}{\lambda\cos\theta}\Im(E_{\text{eff}}),$$

$$\gamma = -\frac{2\pi n^3 r_{\text{eff}}}{\lambda\cos\theta}\Re(E_{\text{eff}}), \quad \tan\phi = \frac{\Gamma}{\gamma}, \tag{6}$$

where n is the average refractive index, r_{eff} is the effective electro-optic coefficient, 2θ is the angle between the incident beams, ϕ is the hologram phase shift, and E_{eff} is the so-called effective field, which for the case of a hologram steadily moving with speed v (detuning frequency Kv) can be written as[7]

$$E_{\text{eff}} = -\frac{E + iE_D}{1 + K^2 l_S^2 - iKl_E - i\tau_M Kv(1 + K^2 L_D^2 - iKL_E)}, \tag{7}$$

with

$$E_D = K\frac{k_B T}{q}, \qquad l_S^2 = \frac{k_B T\epsilon\varepsilon_0}{q^2(N_D)_{\text{eff}}}, \qquad l_E = \frac{\epsilon\varepsilon_0 E}{q(N_D)_{\text{eff}}},$$

$$L_D^2 = D\tau, \qquad D = \mu k_B T/q, \tag{8}$$

$$(N_D)_{\text{eff}} = \frac{N_D^+(N_D - N_D{}^+)}{N_D}, \qquad L_E = \mu\tau E,$$

$$\tau_M = \frac{\epsilon\varepsilon_0 h\nu d}{q\mu\tau\Phi I_{\text{abs}}}. \tag{9}$$

Here only the first spatial harmonics of the space-charge field are taken into account; k_B is the Boltzmann constant, q is the charge of the electron, and T is the absolute temperature. The total density and the density of the ionized photoactive centers are N_D and $N_D{}^+$, respectively, ϵ is the dielectric constant, ε_0 is the vacuum permittivity, and D and τ are the photoelectron's diffusion constant and lifetime, respectively. L_E is the drift length, μ is the photoelectron's mobility, τ_M is the Maxwell relaxation time, d is the crystal thickness, Φ is the quantum efficiency for photoelectron generation at wavelength $\lambda = c/\nu$, and I_{abs} is the absorbed irradiance. As for the case of Eqs. (1) and (2), the factor that accounts for the polarization state of the interacting beams in the expressions for Γ and γ in Eq. (6) is also approximately 1. The optical activity in this material makes this polarization factor in Γ and γ vary along the crystal thickness,[10] but for our thin (2-mm) sample this variation is estimated to be rather small (less than 8%) and can be neglected, unlike the effect of absorption that is analyzed in this paper.

In the present experiment V_Ω is used as an error signal in the negative-feedback optoelectronic loop represented in Fig. 1, so its value is actively fixed to $V_\Omega = 0$. This choice leads to a special class of (fringe-locked) hologram for which $\varphi = 0$.[3] Under this condition we can use the relation $V_{2\Omega} \propto \sqrt{\eta(1-\eta)}$ to follow the evolution of η during recording. From Eqs. (5) and (6) we find that $\varphi = 0$ means that $\gamma d/4 \propto \Re(E_{\text{eff}}) = 0$, where $\Re(E_{\text{eff}})$ can be computed from Eq. (7) as

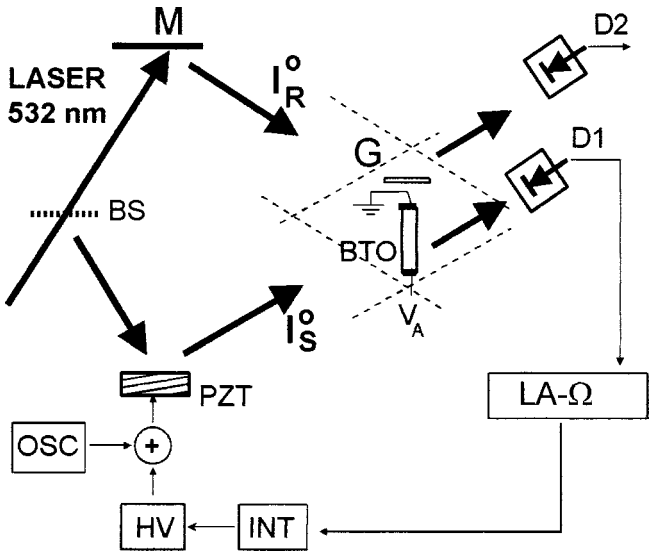

Fig. 1. Experimental setup: G, glass plate; BTO, $Bi_{12}TiO_{20}$ crystal; V_A, applied voltage; D_1, D_2, photodetectors; LA-Ω, lock-in amplifier tuned to frequency Ω; INT, integrator; HV, high-voltage source amplifier driving piezo-electric supported mirror PZT; OSC, oscillator producing the Ω-frequency signal used to modulate the phase of beam I^0_S; BS, beam splitter; M, mirror.

$$\Re(E_{\text{eff}}) = -\frac{E(1 + K^2 l_s^2 - K^2 L_E v \tau_M) - E_D[K l_E + K v \tau_M (1 + K^2 L_D^2)]}{(1 + K^2 l_s^2 - K^2 L_E v \tau_M)^2 + [K l_E + K v \tau_M (1 + K^2 L_D^2)]^2}. \quad (10)$$

From $\Re(E_{\text{eff}}) = 0$ we deduce an expression for the hologram velocity[3]:

$$v = \frac{1}{K \tau_M} \frac{E E_D}{E^2 K^2 L_D^2 + E_D^2 (1 + K^2 L_D^2)}. \quad (11)$$

From Eq. (11) we could compute L_D and τ_M (and related quantities) if absorption effects could be neglected, but that is usually not possible.

B. Bulk Absorption Effect

The dependence of τ_M on the absorbed light in the crystal volume (I_{abs}/d) as shown in Eq. (9) is justified only for when $\alpha d \ll 1$. Otherwise the expression I_{abs}/d should be replaced by

$$-\frac{\mathrm{d}I}{\mathrm{d}z} = \alpha I_0 \exp(-\alpha z), \quad (12)$$

where I_0 is the input incident light intensity. The thickness dependence of τ_M is therefore

$$\tau_M(z) = \tau_M(0) \exp(\alpha z), \quad (13)$$

where $\tau_M(0)$ is the dielectric relaxation time at the crystal front. We conclude also that the effective field of Eq. (7) as well as Γ and γ from Eq. (6), depends on z. It has already been reported[10] and can easily be demonstrated, at least for the undepleted-pump approximation in our case, that the expressions Γd and γd found in the derivation of the intensities and phases of the coupled waves should be replaced by $\int_0^d \Gamma(z)\mathrm{d}z$ and $\int_0^d \gamma(z)\mathrm{d}z$, respectively. In fact, from the well-known coupled-wave equations we can deduce the differential expressions for the intensity (I_S) and the phase (ψ_S) of the complex coupled light amplitude $\sqrt{I_S}\exp(-\psi_S)$ (Ref. 11):

$$\frac{\partial I_S(z)}{\partial z} = \Gamma(z) \frac{I_R(z) I_S(z)}{I_R(z) + I_S(z)}, \quad (14)$$

$$\frac{\partial \psi_S(z)}{\partial z} = -\frac{\gamma(z)}{2} \frac{I_R(z)}{I_R(z) + I_S(z)}, \quad (15)$$

where the explicit dependence of the real [$\gamma(z)$] and the imaginary [$\Gamma(z)$] parts of the coupling constant on the crystal thickness (z) are indicated. For the undepleted-pump approximation ($I_R \gg I_S$), Eqs. (14) and (15) can be simplified to

$$\frac{1}{I_S(z)} \frac{\partial I_S(z)}{\partial z} = \Gamma(z), \quad (16)$$

$$\frac{\partial \psi_S(z)}{\partial z} = -\frac{\gamma(z)}{2}. \quad (17)$$

From Eqs. (16) and (17) it is evident that the coupling of amplitude and phase depends on the integrals of Γ and γ, respectively. That is, the simple products Γz and γz should be replaced by their respective integrals everywhere. Consequently the condition $\Re(E_{\text{eff}}) = 0$ is to be replaced by

$$\frac{1}{d} \int_0^d \Re[E_{\text{eff}}(z)]\mathrm{d}z = 0. \quad (18)$$

Substituting Eqs. (10) and (13) into Eq. (18) and analytically calculating the integral in the latter equation result in the following relation:

$$\frac{\sqrt{4ac - b^2}\,\tau_M(0) K v [\exp(\alpha d) - 1]}{2c + 2a\tau_M^2(0) K^2 v^2 \exp(\alpha d) + b\tau_M(0) K v [\exp(\alpha d) + 1]} = \tan\left(\frac{x\sqrt{4ac - b^2}}{2cg + xb}\left\{\alpha d - \frac{1}{2}\ln\left[\frac{a\tau_M^2(0) K^2 v^2 \exp(2\alpha d) + b\tau_M(0) K v \exp(\alpha d) + c}{a\tau_M^2(0) K^2 v^2 + b\tau_M(0) K v + c}\right]\right\}\right) \quad (19)$$

$$\text{for } 4ac \geqslant b^2, \quad (20)$$

with the following definitions: $a = (K^2L_D^2x)^2 + (1 + K^2L_D^2)^2$, $b = 2x(K^2l_s^2 - K^2L_D^2)$, $c = (1 + K^2l_s^2)^2 + (K^2l_s^2x)^2$, $g = K^2L_D^2x^2 + K^2L_D^2 + 1$, $x = E/E_D$. Note that Eq. (11) is actually the limit of Eq. (19) for $\alpha d \rightarrow 0$. It can easily be verified that the condition in inequality (20) always holds. Equation (19) represents an implicit relation between the detuned frequency Kv and the normalized applied field $x = E/E_D$ that can be calculated numerically. The effective value of the field at the point where measurements are carried out is accounted for by substitution of ξE for E everywhere in Eq. (19), where ξ is the effective field coefficient.[5]

3. EXPERIMENT

A fringe-locked running hologram experiment was carried out with the setup schematically illustrated in Fig. 1. A 2.05-mm-thick nominally undoped photorefractive $Bi_{12}TiO_{20}$ crystal (labeled BTO) was measured in a typical transverse (electric field applied roughly transversally to the laser beam's direction) configuration, with the pattern of light (532-nm laser line) projected onto the (110) plane of the crystal and the wave vector **K** perpendicular to the [001] axis. The beam irradiances were $I_S^0 = 92\ \mu\text{m/cm}^2$ and $I_R^0 = 3.0\ \text{mW/cm}^2$. Their input polarizations were chosen such that the transmitted and the diffracted light behind the crystal was approximately parallel polarized.[12] The absorption coefficient was $\alpha = 8.5\ \text{cm}^{-1}$, and the hologram wave vector value was $K = 5.51\ \mu\text{m}^{-1}$. V_Ω behind the crystal was used as an error signal to operate the feedback, whereas the signal across the small glass plate was used to measure the hologram speed, as already described elsewhere.[6]

Figure 2 shows the experimental data from the fringe-locked experiment and the best fit to the theoretical dependence of Kv on E/E_D as derived numerically from Eq. (19). The fit was carried out with the parameters $L_D = 0.14 \pm 0.01\ \mu\text{m}$ and $l_s = 0.065 \pm 0.005\ \mu\text{m}$, which were obtained from previous phase-shift experiments (similar to those reported in Refs. 4 and 5) that are insensitive to bulk absorption. The best fit leads to $\Phi = 0.36$ and $\xi = 0.73$. The parameters ξ and Φ have rather different effects on the Kv-versus-E curve (the former acts on the width of the curve, whereas the latter acts on the height), and that is why it is possible to find accurate fitting values for both parameters simultaneously. If absorption is not taken into account and the simple formulation in Eq. (11) is used, a different (and erroneous) $\Phi = 0.15$ is obtained. Two other independent fringe-locked experiments were carried out for the same sample and wavelength: one for the same value of K and incident irradiances $I_R^0 = 5.27\ \text{mW/cm}^2$ and $I_S^0 = 0.17\ \text{mW/cm}^2$, and the other for $K = 7.07\ \mu\text{m}^{-1}$ and for roughly 1-order-of-magnitude lower irradiance $I_R^0 = 380\ \mu\text{W/cm}^2$ and $I_S^0 = 22.4\ \mu\text{W/cm}^2$. Both sets of data were fitted with the already known values for L_D and l_s, and the resultant parameters were $\xi = 0.75$, $\Phi = 0.34$ and $\xi = 0.9$, $\Phi = 0.41$, respectively. From the three experiments we got an average $\Phi = 0.37$ with an approximate 10% dispersion. The major cause of this dispersion probably is the difficulty in evaluating the actual irradiance inside the sample because of scattering and multiple reflections. The uncertainties reported above for L_D and l_s were instead shown to have a negligible influence on Φ.

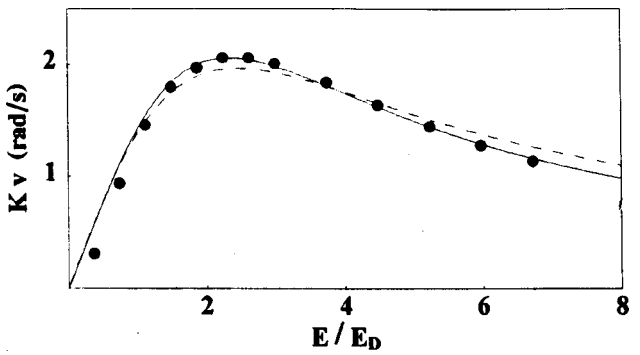

Fig. 2. Experimentally measured detuning Kv measured in a fringe-locked experiment (filled circles) as a function of the ratio of applied to diffusion fields E/E_D. The best fit (continuous curve) to the implicit relations in Eq. (19) leads to $\xi = 0.73$ and $\Phi = 0.36$ for the parameters $L_D = 0.14\ \mu\text{m}$ and $l_s = 0.065\ \mu\text{m}$. The theoretical fit (dashed curve) to the simplified Eq. (11), where absorption is not taken into account, leads to $\Phi = 0.15$ when all other conditions are unchanged.

4. CONCLUSIONS

We have shown that fringe-locked photorefractive running holograms in absorbing materials can be described by an analytical formulation that leads to an implicit relation between the hologram speed and the applied electric field. The quantum efficiency of the charge carriers in these materials can be computed from fringe-locked running hologram experiments with the help of the present formulation, even in the presence of considerable electric field shielding effects. We have also shown that not taking absorption into account may lead to large errors in the computed value of the quantum efficiency.

ACKNOWLEDGMENTS

We are grateful to the Laboratório de Crescimento de Cristais for the good-quality $Bi_{12}TiO_{20}$ crystal that enabled us to perform this research. We acknowledge partial financial support from the Conselho Nacional de Desenvolvimento Científico e Tecnológico, the Fundação de Amparo à Pesquisa do Estado de São Paulo, the Financiadora de Estudos e Projetos (Brazil), and Volkswagen-Stiftung (Germany).

J. Frejlich's e-mail address is frejlich@ifi.unicamp.br.

*Present address, Departamento de Física, Universidade Estadual Paulista, Rio Claro—SP, Brazil.

†Present address, Academia da Força Aérea, Pirassununga—SP, Brazil.

‡Permanent address, Institute of Physics, National Academy of Sciences, 252650, Kiev, Ukraine.

REFERENCES

1. S. I. Stepanov, V. V. Kulikov, and M. P. Petrov, "'Running' holograms in photorefractive $Bi_{12}TiO_{20}$ crystals," Opt. Commun. **44**, 19–23 (1982).

2. G. Hamel de Montchenault, B. Loiseaux, and J. P. Huignard, "Moving grating during erasure in photorefractive $Bi_{12}SiO_{20}$ crystals," Electron. Lett. **22**, 1030–1032 (1986).
3. J. Frejlich, P. M. Garcia, and L. Cescato, "Adaptive fringe-locked running hologram in photorefractive crystals: errata," Opt. Lett. **15**, 1247 (1990).
4. P. M. Garcia, L. Cescato, and J. Frejlich, "Phase-shift measurement in photorefractive holographic recording," J. Appl. Phys. **66**, 47–49 (1989).
5. A. A. Freschi, P. M. Garcia, and J. Frejlich, "Charge-carrier diffusion length in photorefractive crystals computed from the initial hologram phase shift," Appl. Phys. Lett. **71**, 2427–2429 (1997).
6. A. A. Freschi, P. M. Garcia, and J. Frejlich, "Phase-controlled photorefractive running holograms," Opt. Commun. **143**, 257–260 (1997).
7. S. Stepanov and P. Petrov, *Photorefractive Materials and Their Applications I*, P. Günter and J.-P Huignard, eds., Vol. 61 of Topics in Applied Physics (Springer-Verlag, Berlin, 1988), pp. 263–289.
8. E. Shamonina, K. H. Ringhofer, P. M. Garcia, A. A. Freschi, and J. Frejlich, "Shape-asymmetry of the diffraction efficiency in $Bi_{12}TiO_{20}$ crystals: the simultaneous influence of absorption and higher harmonics," Opt. Commun. **141**, 132–136 (1997).
9. J. Frejlich, P. M. Garcia, K. H. Ringhofer, and E. Shamonina, "Phase modulation in two-wave mixing for dynamically recorded gratings in photorefractive materials," J. Opt. Soc. Am. B **14**, 1741–1749 (1997).
10. P. D. Foote and T. J. Hall, "Influence of optical activity on two beam coupling constants in photorefractive $Bi_{12}SiO_{20}$," Opt. Commun. **57**, 201–206 (1986).
11. C. H. Kwak, S. Y. Park, H. K. Lee, and E.-H. Lee, "Exact solution of two-wave coupling for photorefractive and photochromic gratings in photorefractive materials," Opt. Commun. **79**, 349–352 (1990).
12. A. A. Kamshilin and M. P. Petrov, "Continuous reconstruction of holographic interferograms through anisotropic diffraction in photorefractive crystals," Opt. Commun. **53**, 23–26 (1985).